CrossMark

RESEARCH ARTICLE

Sediment plume model—a comparison between use of measured turbidity data and satellite images for model calibration

Amir Sadeghian[1] · Jeff Hudson[2] · Howard Wheater[1] · Karl-Erich Lindenschmidt[1]

Abstract In this study, we built a two-dimensional sediment transport model of Lake Diefenbaker, Saskatchewan, Canada. It was calibrated by using measured turbidity data from stations along the reservoir and satellite images based on a flood event in 2013. In June 2013, there was heavy rainfall for two consecutive days on the frozen and snow-covered ground in the higher elevations of western Alberta, Canada. The runoff from the rainfall and the melted snow caused one of the largest recorded inflows to the headwaters of the South Saskatchewan River and Lake Diefenbaker downstream. An estimated discharge peak of over 5200 m³/s arrived at the reservoir inlet with a thick sediment front within a few days. The sediment plume moved quickly through the entire reservoir and remained visible from satellite images for over 2 weeks along most of the reservoir, leading to concerns regarding water quality. The aims of this study are to compare, quantitatively and qualitatively, the efficacy of using turbidity data and satellite images for sediment transport model calibration and to determine how accurately a sediment transport model can simulate sediment transport based on each of them. Both turbidity data and satellite images were very useful for calibrating the sediment transport model quantitatively and qualitatively. Model predictions and turbidity measurements show that the flood water and suspended sediments entered upstream fairly well mixed and moved downstream as overflow with a sharp gradient at the plume front. The model results suggest that the settling and resuspension rates of sediment are directly proportional to flow characteristics and that the use of constant coefficients leads to model underestimation or overestimation unless more data on sediment formation become available. Hence, this study reiterates the significance of the availability of data on sediment distribution and characteristics for building a robust and reliable sediment transport model.

Keywords South Saskatchewan River · Lake Diefenbaker · Sedimentation · Erosion · Satellite images · MODIS · CE-QUAL-W2

✉ Amir Sadeghian
amir.sadeghian@usask.ca

1 Global Institute for Water Security and School of Environment and Sustainability, University of Saskatchewan, 11 Innovation Boulevard, Saskatoon, SK S7N 3H5, Canada

2 Global Institute for Water Security and Department of Biology, University of Saskatchewan, Saskatoon, SK, Canada

Introduction

We are facing more demands and competition for the use of water resources every day and, at the same time, are confronted with greater uncertainties when attempting to predict future conditions (Wheater and Gober 2013). Uncertainties can be especially numerous when trying to accurately predict floods (Horritt 2006; Pappenberger et al. 2006), while they are becoming more frequent due to climate change (Bolstad 2016; Wheater and Evans 2009). Flood peaks lead to high erosion rates and, consequently, high suspended sediments and turbidity in surface waters (Grove et al. 2013). Suspended sediments (SS) contribute to the turbidity of the water and change density and nutrient availability, as well as attenuating the effects of sunlight which protects pathogens from UV radiation (Ji 2008). Suspended solids are also an important carrier of pollutants to lakes and reservoirs (Kroon et al. 2012). Contaminants adsorb to SS surfaces and can be transported hundreds of kilometers with the water flow

🌍 Springer

(Surbeck et al. 2006). Phosphorous, which is the main limiting nutrient for eutrophication in freshwaters, also bonds strongly with SS and is transported when there are high erosion rates which can cause water quality problems. Extensive sediment deposition and siltation lead to expensive maintenance costs and may impede or hinder navigation (Liu et al. 2011). Extensive siltation in a reservoir can decrease the operational lifespan of the waterbody and become an ecological problem itself (Valero-Garces et al. 1999). Also, accumulated loads of sediment behind the dams can increase dam instability because of the excessive forces applied to the dam walls by the sediment loads (Mama and Okafor 2011). Hence, more money and resources are expended to mitigate the impacts of climate change and research new approaches for adaptation (Derworiz 2016).

Floods can bring significant amounts of suspended solids to lakes and at the same time change the mixing patterns in lakes by turbulence currents. The effects of vertical mixing are dependent on the direction of water exchange in lakes. Depending on the inflow water density gradient (a function of water temperature and dissolved and suspended solids), the incoming flow could enter the reservoir in three different ways (Romero and Imberger 2003). Warmer river waters usually have a lower density than the lake's water and enter along the top of the lake's surface as overflow (Ji 2008). The heavier river waters, which are mainly due to cold and sediment-laden flood waters, enter along the lakebed as underflow or density currents (Fink et al. 2016). At the point where the density of the underflow becomes lower than the density of the water at the lakebed, the flow spreads into the upper layers as interflow until the mixing balances the density gradient (Alavian et al. 1992).

The intrusion of the nutrient-rich hypolimnion water with the oxygen-rich epilimnion water can increase the productivity, while the reverse would reduce the oxygen deficiency and even lead to hypolimnetic oxygen saturation (Wüest et al. 1988). Large quantities of suspended solids can influence the water quality by changing the sediment-water interactions and the ecological balance (Walling 1977). In an incident in August 2002, the channel walls in the Mulde River, Germany, broke during a severe flood and the nutrient-rich water drained into nearby stratified pit lakes (Klemm et al. 2005). The flood caused oxygen depletion in the epilimnion and the occurrence of algal blooms in these oligotrophic to mesotrophic lakes, which was of concern regarding the water supply (Boehrer et al. 2005).

The floods are also essential for renewal of water in deep layers of lakes and reservoir and can even reduce eutrophication (Fink et al. 2016). Springtime flood water has a higher density than lake surface water because of lower water temperatures and higher concentrations of suspended solids, hence transporting the oxygen-rich water along lake's bottom (Fink et al. 2016). In a study of the Rhine River/Lake Constance, Germany, it was found that the spring-time underflow floods renew about 27% of the hypolimnion water with oxygen-rich water every year, which is essential to maintain higher quality of the water in deep areas (Fink et al. 2016). In Lake Burragorang, Australia, winter flood completely replaces the anoxic hypolimnion with the underflow (Romero and Imberger 2003). A study on Lake Rotoiti, New Zealand, found that, depending on the timing and flow characteristics, the density-driven underflow has both positive and adverse effects on the ecological dynamics, nutrient loading, dissolved oxygen concentration, and eutrophication on this lake (Vincent et al. 1991).

Even the best-controlled floods can be subject to the abovementioned potential environmental and ecological impacts by transported suspended solids. At such time, key questions and concerns require accurate and quick answers, such as the amount of sediment and pollutants transported through flooding, the effect of the sediment plume (e.g., contamination), bacterial counts, safety of recreational beaches, and the need for drinking water advisories.

Answering these questions is not easy and becomes even more complicated as we go forward in an uncertain future. Water quality models are useful tools for studying the physical, chemical, and biological processes and mechanisms in rivers and lakes (Sadeghian et al. 2014). Modeling SS transport can provide valuable information on contaminant transport characteristics and rates (Langeveld et al. 2005). In this study, we built and calibrated a sediment transport model based on the largest recorded flood for Lake Diefenbaker (LD), since its impoundment in 1967, in the prairie province of Saskatchewan, Canada.

The primary factors affecting the characteristics of a reservoir include climate, soil mineralogical composition, vegetation, land use, and management practices in the watershed (Wetzel 2001). Also, the topography of the region regarding the solar radiation shading and the wind speed sheltering are important (Huber et al. 2008). The heat exchange at the surface by solar radiation and the wind forces on the surface provide a significant proportion of energy for mixing in the lakes (Wüest et al. 1988). In Lake Diefenbaker, the energy from the inflow also has considerable effects on the mixing and horizontal water movements (Sadeghian et al. 2015).

In June 2013, there was heavy rainfall for two consecutive days on the frozen and snow-covered ground in the higher elevations of western Alberta, Canada (Sutherland 2016). The runoff from the rainfall and melted snow caused one of the largest recorded inflows to the headwaters of the South Saskatchewan River (SSR) and caused heavy damage to population centers, particularly High River and Calgary, and devastation in the surrounding areas (De Vynck and Polson 2013; Welsch and De Vynck 2013). The gauges recorded discharge with peaks of 4500 m³/s at the Medicine Hat station (SSR) and 950 m³/s at the Bindloss station (Red Deer River (RDR)),

which merge at the Alberta-Saskatchewan border, 171 km from the Lake Diefenbaker inlet. Lake Diefenbaker, located downstream, was formed by the construction of the Gardiner Dam and the Qu'Appelle River Dam in the 1960s (Fig. 1). Similar to many reservoirs, Lake Diefenbaker also functions as a flood mitigation reservoir. The 2013 Alberta flood brought highly turbid water into the reservoir (Hudson and Vandergucht 2015), where the sediment settling and resuspension rates were unknown, leading to concerns regarding water quality.

We used measured turbidity data collected from stations along the reservoir over the course of 2 months (June and July 2013) to validate the sediment model quantitatively. In a sediment transport model, the use of suspended solid (SS) concentrations is preferred over turbidity because it is a state variable in the model, while the turbidity needs to be converted to SS for comparisons. However, a fundamental limitation with SS is maintaining a consistent sampling program of sediment with a temporal frequency that is adequate to capture the variations between seasons and events such as floods (Stroud et al. 2009). The acquisition of data, from which decisions are often based, is frequently inadequate, and this may lead to underestimation or overestimation and, ultimately, to poor management and policy decisions (Littlewood 1992). Therefore, a practical alternative is using turbidity measurements (Gippel 1995). Sonde-based turbidity measurements correlate the light scattering in water with SS concentrations, and are easier, faster, and less expensive to operate compared with suspended solid sampling. Hence, sondes provide SS readings at finer temporal and spatial scales. The results will be very close to the direct measurements when the sensors are calibrated properly, according to particle size variations (Gippel 1995).

In addition, we used MODIS satellite images to qualitatively calibrate the model based on near-surface suspended solids and to track the sediment plume front. Use of satellite images is not a new technique in studying near surface conditions in waterbodies. They are being used in two primary fields: phytoplankton-dominated systems, which are based on absorption of light at the water surface, and inorganic sediment systems, which are based on scattering of light at the water surface (Budd and Warrington 2004; Myint and Walker 2002). The focus of this study is the second category. Turbid waters exhibit strong relationships between sediment concentrations and reflected bands because the SS properties, such as particle size distribution, exert considerable control over the reflectance and scattering (Binding et al. 2005). One of the most comprehensive studies on freshwater, in this context, is the study of sediment transport and resuspension in Lake Michigan, which was accompanied by an extensive data collection project entitled "Episodic Events Great Lakes Experiment (EEGLE)" (Cardenas et al. 2005; Eadie et al. 2002; Lee et al. 2005, 2007; Stroud et al. 2009). Sakmont Engineering (1987) was one of the first groups who looked at satellite images of the SSR Basin and suggested incorporation of NOAA-VHRR and LANDSAT images for consistent data with reasonable resolutions. For Lake Diefenbaker, the first use of satellite images was in estimating chlorophyll *a* concentrations using MODIS and LANDSAT data (Giesy et al. 2009), with further work completed by Hecker et al. (2012) and Yip (2015).

Lake Diefenbaker is a long (180 km) and narrow reservoir where the width increases from about 800 m upstream to about 4000 m downstream. MODIS data with the finest resolution (i.e., 250 m) would have 3 pixels for the upstream part and about 16 pixels downstream. The chlorophyll *a* concentrations are generally higher downstream, and the upstream area is more light limited because of higher SS concentrations (Dubourg et al. 2015). Therefore, studies based on the use of satellite images were mainly concentrated on estimating

Fig. 1 Lake Diefenbaker (LD), Saskatchewan, Canada. The reservoir is divided into four sections (waterbodies) which allow use of four different meteorological stations along the reservoir. *Solid red lines* show locations of waterbodies in the model. The *dotted red line* at the Elbow shows the location at which the Qu'Appelle River Dam branch merges to the main lchannel in the model. *Red circles* show locations of stations with turbidity data
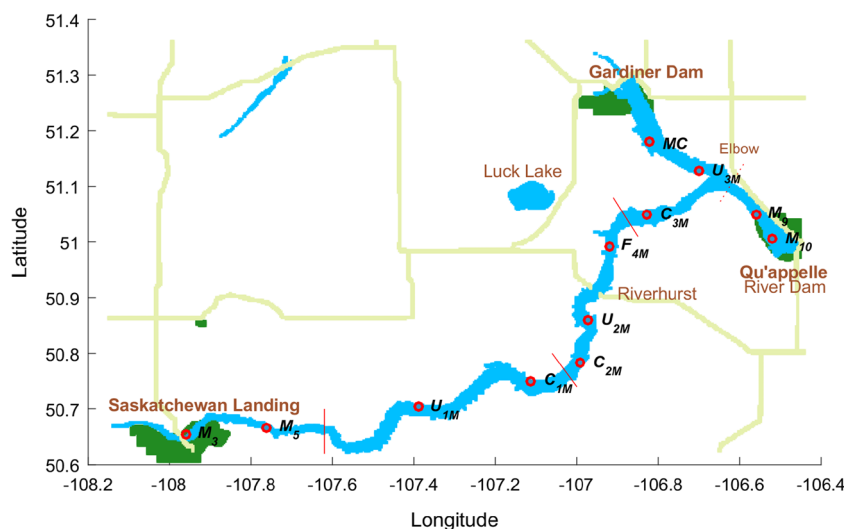
chlorophyll *a* concentrations downstream. We could not find any study that correlates SS or turbidity data with reflectance bands from satellite images for Lake Diefenbaker.

A recent research study by Akomeah et al. (2015) conducted a modeling study of the nutrient-algal dynamics of the upper SSR; due to the high importance of this waterbody to the province of Saskatchewan, we are presenting an extension to that study by looking at the sediment transport characteristics using recorded satellite images, onsite turbidity measurements, and numerical modeling. In this paper, we successfully demonstrate a sediment transport modeling for the largest recorded discharge to Lake Diefenbaker, an important drinking water source, with the objective of reproducing the measured turbidity data quantitatively and reproducing the movement of the sediment plume front qualitatively. A novelty of this work is incorporating space-borne remote sensing data to calibrate the sediment plume progression through the reservoir. The model itself has a sensitivity analysis component for finding the most important parameters that influence the accuracy of the results.

Methods

Study site

The study covers the 2-month period of June and July 2013, and the study area is Lake Diefenbaker (LD). Lake Diefenbaker is one of the most strategic sources of water in the prairie province of Saskatchewan, Canada. The reservoir is 182 km long, with about 98% of its inflow coming from the headwaters of the Rocky Mountains in Alberta. The average annual inflow to the reservoir is 170 m^3/s of which 95% is released from the dams to downstream rivers. The South Saskatchewan River (SSR) and Red Deer River (RDR) merge about 171 km from the Lake Diefenbaker inlet. The closest stations to the reservoir that measure the discharge and suspended solids are the Medicine Hat station, 203 km upstream of the confluence for the SSR, and the Bindloss station, 47 km upstream of the confluence for the RDR. The SSR has a 50-year average flow of 550 m^3/s for June and 271 m^3/s for July, with a minimum flow of 8.5 m^3/s in November 1984 and a maximum of 4440 m^3/s in June 2013. The RDR has a 50-year average flow of 135 and 122 m^3/s for June and July respectively, with a minimum flow of 2.2 m^3/s in November 1982 and a maximum of 984 m^3/s in June 2005. The second and third largest recorded flows for the RDR are 932 and 928 m^3/s in June 2013. Figure 2 shows the inflow and outflow to and from Lake Diefenbaker based on the routed discharges of the SSR and RDR, according to the methodology described in Hudson and Vandergucht (2015).

The air temperature ranged between 5 and 35 °C with mostly clear skies in June and July 2013 (Fig. 3). The wind

had a maximum velocity of about 11 m/s and was faster than 6 m/s for 10% of the time during this period, which could cause fairly strong mixing up to several meters below the surface. The heat budget for water temperature in Lake Diefenbaker has two main sources: heat from inflow water, which is transported longitudinally by advection, and energy at the surface from solar radiation, which is distributed vertically by wind forces (Sadeghian et al. 2015). Modeling studies by Sadeghian et al. (2015) show that at the time when the flood peak arrived at the reservoir, there was a fairly distinct stratification, with the thermocline about 20 m from the surface (Fig. 4).

Measurements

The turbidity measurements were collected using YSI 6600 v2 multi-parameter sonde for 12 locations along the reservoir (Fig. 1), with two or three vertical profiles for each station during the study period in June and July 2013 (Fig. 5). The upstream stations had turbidity values several orders of magnitude higher than the downstream stations. The values obtained prior to the flooding (June 5) almost doubled after the flood peak arrived at the reservoir (July 4). Further downstream, the turbidity increased up to 20 times after the flood peak. The reservoir bifurcates near the village of Elbow into two 20-km arms. For the stations along these two arms (MC, M_8, M_9, and M_{10}), maximum turbidity values rarely get close to 4 nephelometric turbidity units (NTU) even after the flood.

Satellite images were acquired using MODIS (Terra/MODIS 2013/155-243, bands 1-4-3 (true color), pixel sizes 250 m) for this period. In total, there were 16 images that were available for June and July without having a cloud cover over the reservoir. For the missing days, we linearly interpolated between two available maps. Each pixel (i.e., 250 m) in the image consists of values for three color bands (red, green, and blue (RGB)). For example, the RGB values for a pixel upstream for the 4th of June are [102, 89, 55] and for the 7th are [104, 94, 64]. In order to reproduce the images for the missing days, the 5th and 6th, we interpolated for each of the RGB values separately. In Fig. 6, the days that have data are shown in green and the days that are estimated based on linear interpolation are shown in red. Each image has 400,000 pixels of which 10,555 are for Lake Diefenbaker amounting to about 2.5% water and the most of the remainder is land surfaces. The arrows in each image show the estimated sediment front for each day.

Fig. 2 Discharge values at South Saskatchewan River (SSR), Red Deer ▶ River (RDR), inflow to Lake Diefenbaker (LD), outflow from LD, and water level elevation at the Gardiner Dam. The SSR and RDR merge 171 km upstream of the LD inlet
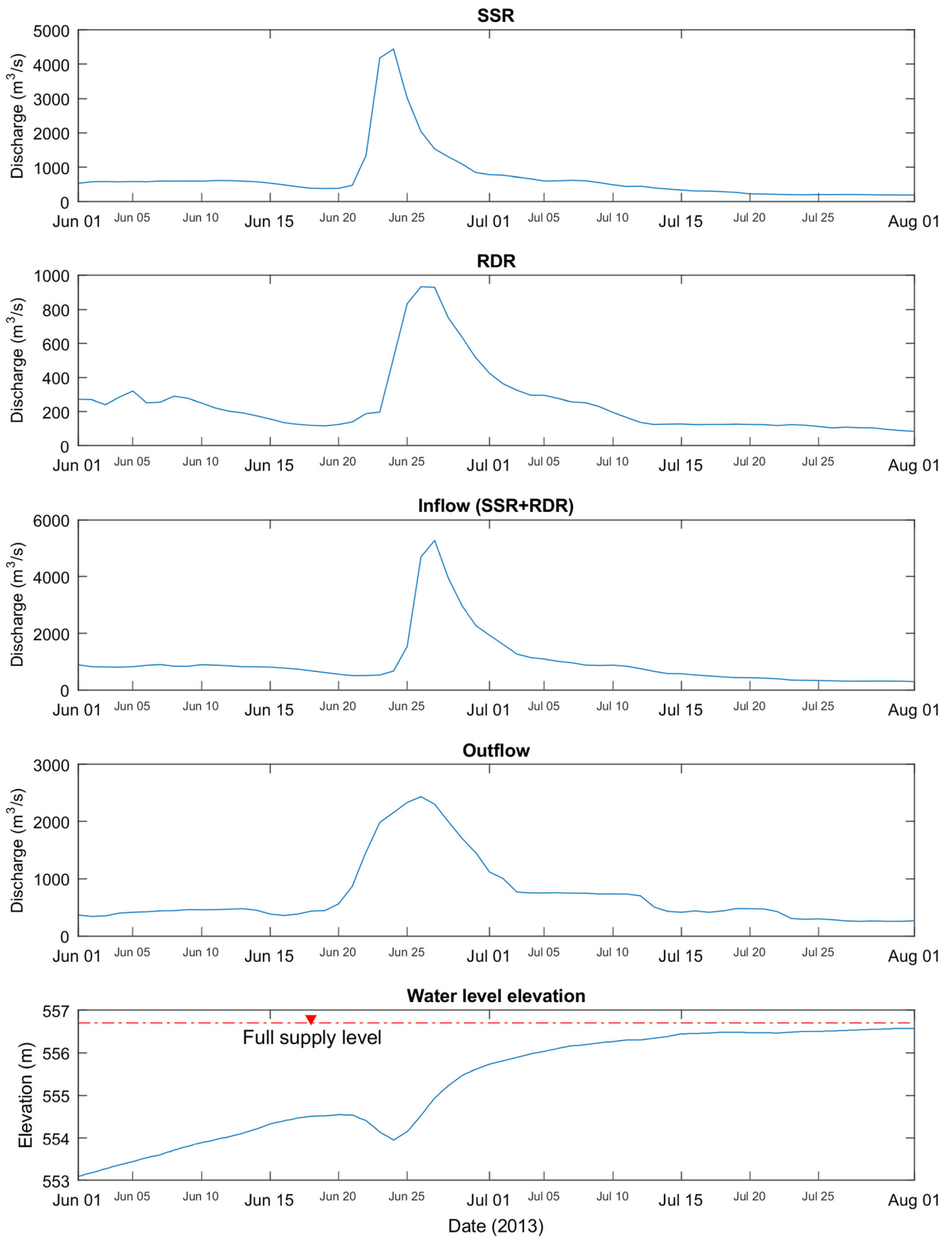
Fig. 3 Recorded air temperature (*top*) and wind speed (*bottom*) at the Elbow station. The *vertical strips* show cloud amount with *darker bands* meaning more clouds
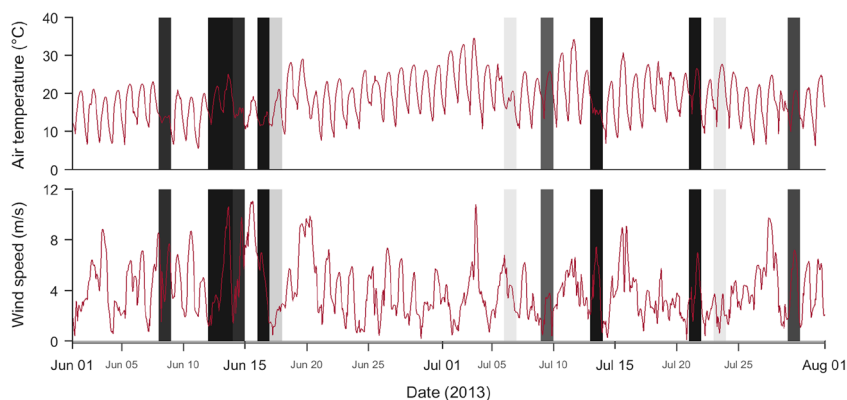
Model

We used the laterally averaged water quality model, CE-QUAL-W2, for this study. This model was initiated in 1975 by the US Army Corps of Engineers and was then developed for about 10 years by Edinger and Buchak (Buchak and Edinger 1984; Edinger and Buchak 1975, 1978) and then for more than 20 years by Cole (Cole and Buchak 1995; Cole and Wells 2003a, 2003b, 2006). Further development is now being continued at Portland State University by Wells and his team (Cole and Wells 2008, 2013, 2015a, 2015b).

CE-QUAL-W2 is capable of performing both hydrodynamic and water quality simulations for both rivers and reservoirs. CE-QUAL-W2 was previously calibrated for temperature and hydrodynamics of Lake Diefenbaker for the 2011–2013 period (Sadeghian et al. 2015). Also, a sensitivity analysis for choosing the best meteorological stations from three available databases (Environment Canada, AccuWeather, and MeteoBlue) was carried out for 2011–2013 using this model. The model can simulate several groups of suspended solids for consideration of the effects of different sediment sizes and compositions. The model uses adoptive timesteps by calculating the Courant number for each step, with a maximum

allowed timestep of 360 s for model stability. Inputs to the model are hourly meteorological data and daily flow and TSS data.

The model setup consists of 300 longitudinal segments, in Cartesian coordinates, ranging from 300 to 950 m in length, and 60 uniform vertical layers with a thickness of 1 m each. Also, the reservoir is divided into four waterbodies, connected to each other as shown in Fig. 1. The inclusion of several waterbodies enables the use of different climate data stations for a large domain, as well as the implementation of different rates and constants for geomorphologically different river and lake sections. Each waterbody has one main branch, to which several side branches can be connected. The additional branches define a slope or connect a stream to the main river. For example, one extra branch connects the Qu'Appelle arm to the main stream at the downstream region of the reservoir.

We started the model simulations at the beginning of April 2013, as we could assume an isothermal condition for the whole reservoir just after the snow cover melted on the reservoir's surface. The model has a warm up period of about 2 weeks, so the effects of initial conditions had completely disappeared for the study period in June and July. Also, all the suspended solids transported to the reservoir by flood were

Fig. 4 Water temperature on July 1, 2013, in Lake Diefenbaker when the flood peak arrived at the reservoir
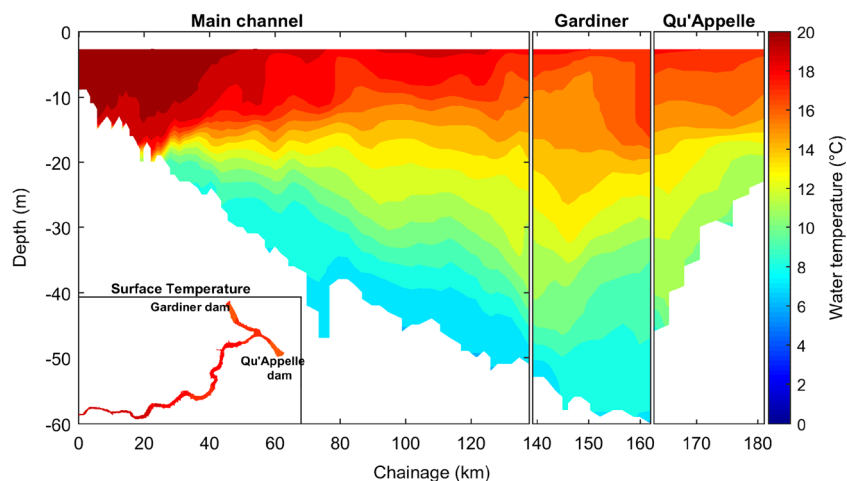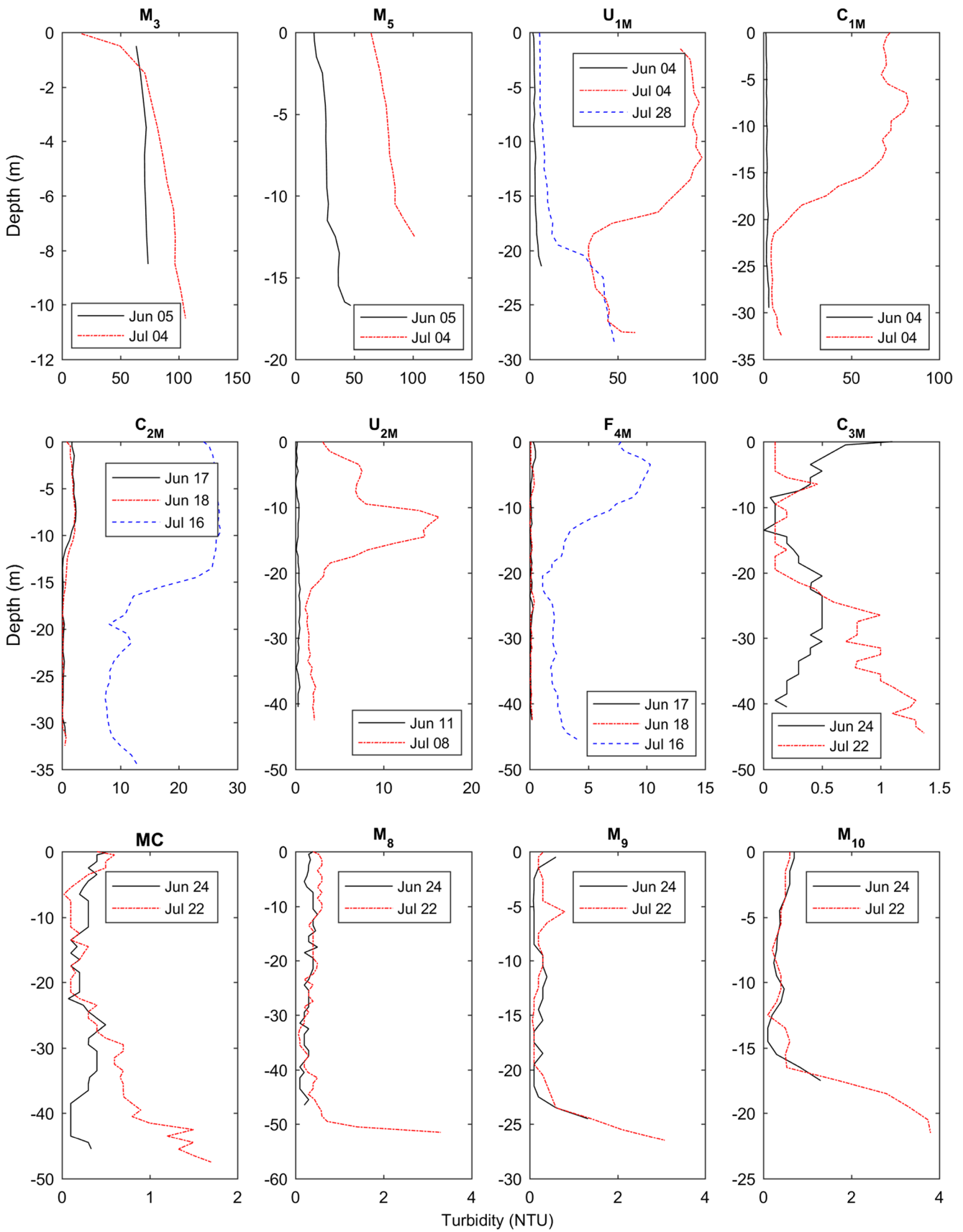
Fig. 5 Vertical turbidity profiles collected at 12 stations along Lake Diefenbaker in June and July 2013
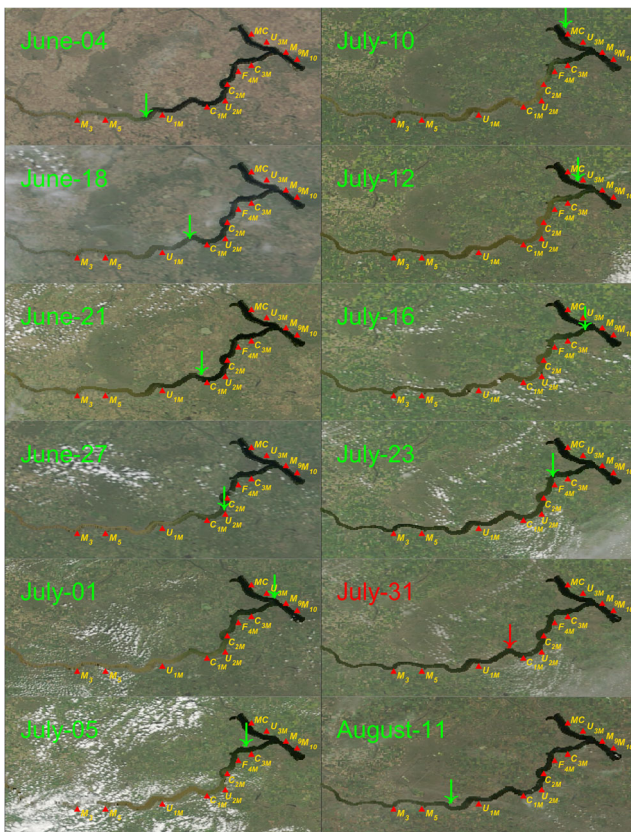
Fig. 6 Satellite images obtained from MODIS for Lake Diefenbaker during the 2013 flood event. Land areas around Lake Diefenbaker blurred by 70% to better show the reservoir area. The images with *green marker* and date are real satellite images. The image with *red marker* (July 31) is interpolated

assumed to be inorganic. Therefore, other modules (e.g., eutrophication) in the model were kept inactive to save computational expenditure. Data from sediment traps were not available to correlate the turbidity measurements with the corresponding total suspended solid (TSS) concentrations. Although there are many studies available that provide guidelines for converting the turbidity measurements into TSS concentrations, we were hesitant in using these resources. The main reason was the data ownership and license limitations
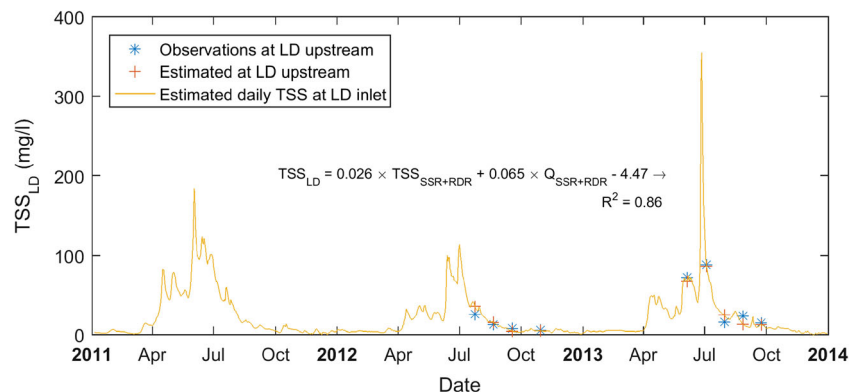
that prevented us from working directly on the data. Hence, to avoid estimation errors and provide a clear path for applying corrections in future studies, the turbidity data (NTU) were considered to be equal to TSS (1 NTU = 1 mg/l). For the same reason, only one class of sediment was considered in the model.

To save computational time, we routed discharge and estimated the TSS value for the upstream portion of LD instead of running the model for the whole SSR + LD domain. The discharge was routed based on available guidelines (Hudson and Vandergucht 2015). Also, a first-order polynomial fitting ($R^2 = 0.86$) between TSS and discharge at the lake's inflow provided a means of extending the TSS measurements to Lake Diefenbaker's upstream stations. A good relationship was also obtained between the TSS concentrations of the LD upstream stations and the discharge and TSS values along the SSR and RDR (Fig. 7). We cannot accurately detect how much TSS the SSR and RDR each contribute to LD because of the distance between observation stations and the reservoir's inlet. The first observation station is about 171 km downstream of the SSR and RDR confluence, but based on the derived equation, about 80–96% of the TSS settled on arrival at LD under normal flow conditions. However, in the 2013 flood, 77% of the sediment had already deposited.

The primary factors that influence the suspended solid concentration in Lake Diefenbaker are the inflow, lake hydrodynamics, sediment concentrations at the inflow (advection), erosion, and sediment resuspension of bed material. Two adjustable model parameters (constant) control the concentration simulations: the suspended solid settling rate (SSS) and the critical shear stress for sediment resuspension (τ_{cr}). The SSS removes suspended solids from the water column and deposits them along the river bottom, while the τ_{cr} resuspends them back from the bottom sediment to the water column. The SSS also serves a critical role in removing particulate phosphorus adsorbed on the SS surfaces; τ_{cr} in return, influences resuspension of nutrients bonded to sediments. The calibrating parameter SSS has a fixed rate expressed as meter per day regardless of flow characteristics. Shear stress at the water-sediment surface is calculated in each timestep based on the

Fig. 7 Estimating the TSS concentration at LD upstream based on C_{IN} and discharge

near bed turbulences induced by the flow and wind effects, but the τ_{cr} has a fixed value for each TSS group during simulations.

In total, 1000 Monte Carlo runs were carried out with uniform distribution for the two calibrating parameters (SSS and τ_{cr}) using the University of Saskatchewan high-performance computing (HPC) platforms. TSS was the primary state variable in our simulations for this study. The settling rate (SSS) and the critical shear stress for sediment resuspension were used to calibrate TSS concentrations by giving the lowest discrepancy with measured turbidity data. Calibrations and sensitivity analysis were performed by optimizing the objective function, root-mean-square error (RMSE):

$$RMSE = \sqrt{\frac{\sum(O-S)^2}{n}} \qquad (1)$$

where O is the observed values, S is the simulated values, and n is the total number of observations.

Calibration of the model, based on the lowest deviation between simulations and measurements within a Monte Carlo environment, has already been described in depth for the Lake Diefenbaker temperature model (Sadeghian et al. 2015). For each Monte Carlo run, we calculated the RMSE based on Eq. 1. To calculate the RMSE for the entire reservoir, all the turbidity measurements from all different depths and locations were sorted in one column and compared with the simulated values at the same place and depth. To calculate the RMSE values for each segment (observation station), only values of that portion filtered to a similar time and depth were considered.

Results

Initial processing of the satellite images revealed that the upper portion of Lake Diefenbaker (up to station M_5) was visibly turbid even before the flood because of high flows in June (Figs. 2 and 6). The plume gradually moved through the reservoir and reached the Riverhurst area by June 27, just before the arrival of flood waters. On July 1, after the flood water arrived at the reservoir, there was a jump in the plume front's location to Elbow. By July 5, the plume disappeared and again extended up to the Gardiner Dam on July 10. Then, it took about 1 month for the plume to disappear completely from the satellite images.

The turbidity measurements also confirm the trends in water clarity visible from satellite images. Before the flood waters entered the reservoir, the vertical profile of turbidity, especially upstream, had higher concentrations near the bed. The vertical profiles for the first two stations (M_3 and M_5) show higher concentrations near the bed, which could be due to sediment resuspension from high discharge values.

However, this trend reversed, excluding upstream, once the peak discharge passed through the reservoir, with more cloudy water near the surface (Fig. 5). The values obtained prior to the flooding (June 5) almost doubled after the flood peak arrived at the reservoir (July 4). Further downstream (U_{1M} to F_{4M}), with increasing reservoir depth, sharp changes in the concentrations are visible at depths around 20 m from the surface. The turbidity measurements recorded immediately after the flooding show up to 20 times increase in turbidity values above the first 20 m from the water surface (on the top of the thermocline). The reason could be that in shallower upstream areas (about 10 m deep), advection and resuspension are the main sources of sediment, while further downstream, it is only advection. These regions had clear water before the flood and the sediment plume increased the turbidity of the water here. The reason for higher turbidities in only the first 20 m could be due to the summer stratification and also be an indication of overflow conditions. The reservoir bifurcates near the village of Elbow into two 20-km arms. For the stations along these two arms (MC, M_8, M_9 and M_{10}) and the C_{3m} station (before branching), maximum turbidity values rarely get close to 4 NTU even after the flood. It is likely that all the SS settled down when it passed through the curvy and indented channel of the reservoir. Resuspension became negligible in deep areas and also because there was overflow conditions.

Among the 27 turbidity measurements (Fig. 5), two thirds had concentrations of less than 15 NTU, which indicated almost clear water. Most of these samples were collected from downstream areas where most of the turbulence energy of the water had dampened. The simulations on these days/stations produced smaller RMSE errors when compared with the other remaining days/stations. Also, the model results were more satisfactory with settling rates (SSS) greater than 2 m/day for suspended solids at these low turbidity events (Fig. 8). The days/locations that had higher turbidities were sensitive to the values of calibrating parameters. Therefore, the results for turbidity observations with a maximum recorded turbidity of over 15 NTU will be discussed in more detail.

Overall, the Monte Carlo simulation results show high sensitivity to SSS values, but no detectable trend was found with τ_{cr} (Fig. 8). A general trend for SSS is that the best results upstream were derived with small values, as we go downstream, the results get better with larger settling rates. On one occasion, U_{1M} on July 4, there are two optimum values for the SSS coefficient. The main reason is the vertical profile of turbidity at this day/location (Fig. 5). There was high turbidity that arrived at the top of the thermocline, while the area below was still clear because of pre-flood clear water conditions. The two optimum values are for two different simulated vertical profiles of which one of them is a false optimum value. This equifinality occurs when the model predicts large concentrations below the thermocline and small values on the

Fig. 8 Sensitivity analysis for parameters SSS (m/day) and τ_{cr} (dynes/cm^2) for observations with TSS values larger than 15 mg/l. SSS ranged between 0 and 6. τ_{cr} ranged between 0 and 4
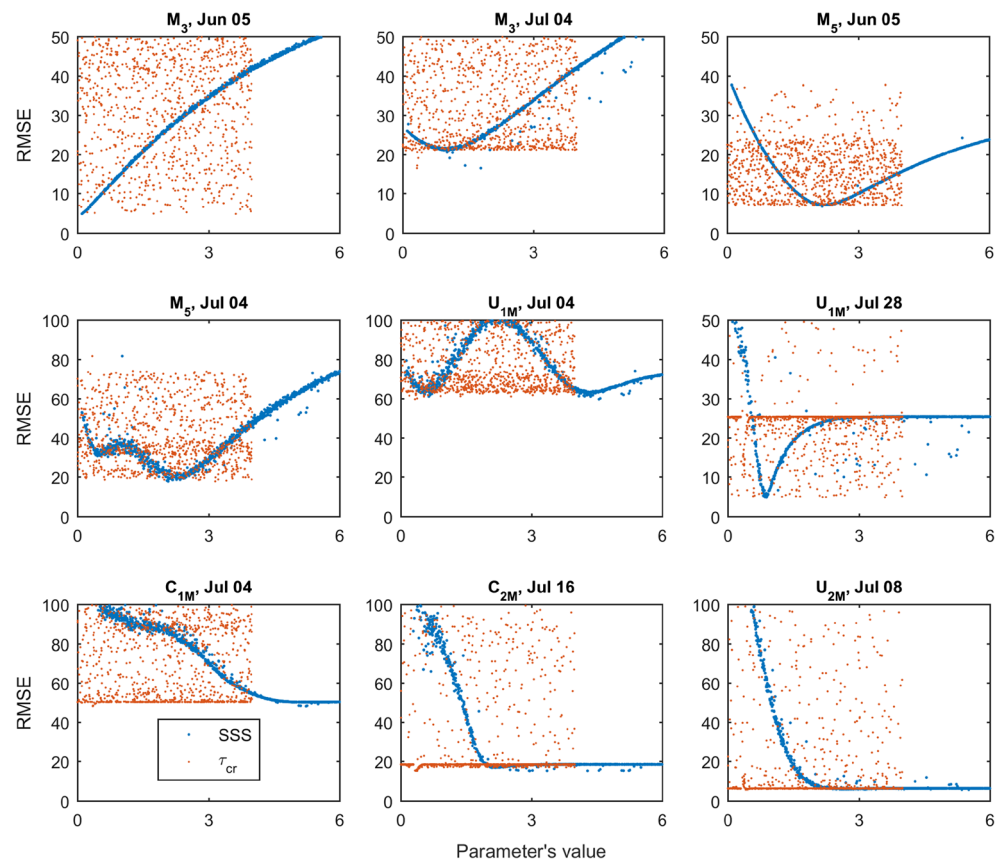
top (inverse profile). The sum of underestimation at the top of the thermocline (negative values) and overprediction below the thermocline (positive values) gives small RMSE values which are not correct. According to the RMSE values, the best results were obtained when SSS increased from 1 to 5 m/day from upstream to downstream in the reservoir.

We chose four different ranges for SSS to look at the results in more detail (Fig. 9). The bands show the ranges that the model calculated for TSS for days/locations by SSS values in the specified ranges. SSS values in the range between 0 and 0.5 m/day produce the best match with the observed turbidity data for station M_3 upstream. The same range overpredicts the TSS by about four times at M_5 and about 15 times at U_{2M}. The range between 1 and 1.5 underestimates the TSS at M_3 before the flood, but works well for the period of the time after the flood. However, it still overestimates at stations more downstream. Larger SSS values underestimate TSS upstream, but are better matched with observations downstream.

Comparing model results at the surface with sediment movement detected in satellite images shows that the value of 6 m/day was a large upper band for SSS (Fig. 10). Almost all the sediment was removed from the top layer by 10 days after the incident, while the images recorded that the surface water upstream was turbid until the end of July. At the same time, SSS values smaller than 1 m/day produced very large concentrations (TSS over 100 mg/l) downstream, which are

not correct. No observation or satellite image confirms such high turbid conditions downstream.

Discussion

In 2013, the Alberta flood had a peak flow of 5200 m^3/s with a maximum TSS concentration of 1500 mg/l at the SSR-RDR confluence (171 km upstream of LD). Dam operation authorities released the water from the Gardiner Dam at a rate of 2000 m^3/s for three consecutive days (Saskatoon City News 2013). Due to the high inflow and outflow, the sediment plume traveled through the reservoir very quickly. Saskatchewan's Water Security Agency reduced the dam's outflow to 1000 m^3/s on the third day when the inflow decreased to less than 2000 m^3/s. As a result, the sediment plume began settling gradually. Based on our modeling results, the inflow water from the SSR had a temperature close to the temperature of the water at the surface of Lake Diefenbaker. Although most of the flow waters stemmed from snowmelt, warm days with extensive sunshine hours (~17 h in June) had brought enough thermal energy to the river. Hence, water entered the lake above the colder and heavier lower layers because of density gradients. However, the large inflow (5200 m^3/s) to the reservoir and the large outflow through the spillways at the Gardiner Dam (2000 m3/s) induced high

Fig. 9 Simulated TSS ranges for different SSS (m/day) values. The *bands* show the ranges that the model calculated the TSS concentrations by using the SSS values in the specified ranges for different days/locations. Small SSS overpredicts TSS at downstream several orders of magnitudes
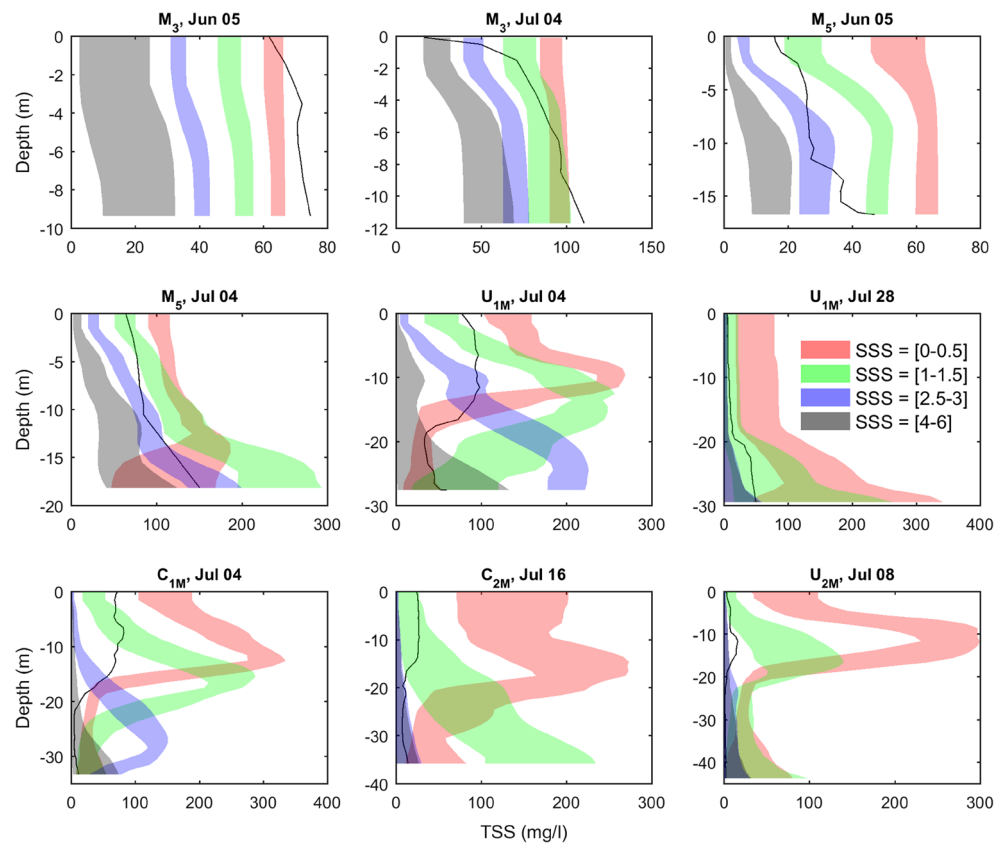
velocity water in transit with large turbulent mixing especially at the upstream sections. Also, during the flood of June, the water level in Lake Diefenbaker raised about 3 m (Fig. 2). According to the recorded water level elevations, there was a rapid drawdown of about 1 m before the flood arrival in June 25 because of the opening of the spillway gates at the Gardiner Dam. According to the model results, the inflow water from SSR thoroughly mixed with the upstream reservoir water and then traveled along the top of thermocline due to density gradients. Hence, the elevated water level added to the epilimnion thickness.

We used two different sources to calibrate the sediment transport model: comparing the movement of the plume through the reservoir with the acquired satellite images and comparing the observed turbidity measurements with TSS. These comparisons had an interesting result in that the coefficients for the best performance based on satellite images were very close to those based on turbidity measurements.

The turbidity measurements recorded immediately after the flooding show the peaks occurred in the first 20 m from the water surface (on the top of the thermocline), which was also confirmed by the model results. Therefore, the satellite images of the surface of the water are an accurate representation of the sediment plume movements. The satellite images show consistent movement of the turbid front of water through Lake Diefenbaker in June. On July 1, the flood waters arrived at the

reservoir, and the movement was faster than in June for a few days, but the plume disappeared in the image recorded on July 5. On the image recorded on July 10, the plume moved forward again. Unfortunately, there is no turbidity measurement between these two dates in the downstream portion, but the changes in the flow intensities can verify this back and forth movement. As mentioned above, there was a huge inflow into the reservoir and large outflows from the dam, which both decreased considerably from the third day after the arrival of the flood waters. The rapid change in flow intensities could create backflow conditions with hypolimnetic mixing. Also, there were huge wind velocities on the 4th of July, which could have further increased the hypolimnetic mixing there.

C-QUAL-W2 was able to track the changes in turbidity only moderately well when fixed coefficients were considered for sediment settling. We cannot clearly say that it was a limitation with the model or with the data. A limitation of the CE-QUAL-W2, and indeed many water quality models, is the use of fixed rates for the parameters in simulations of the state variables. These rates are used in many equations related to transport, hydrodynamics, or water quality. For example, using fixed daily rates for sediment settling produces overestimations and underestimations, depending on flow conditions. Hence, it may be difficult, if not impossible, to obtain simulations that coincide exactly with the values obtained

Fig. 10 Simulated TSS values at the water surface for different SSS (m/day) values. The *color bar* is in logarithmic scale to capture trends in both upstream with large TSS concentrations and downstream with small concentrations
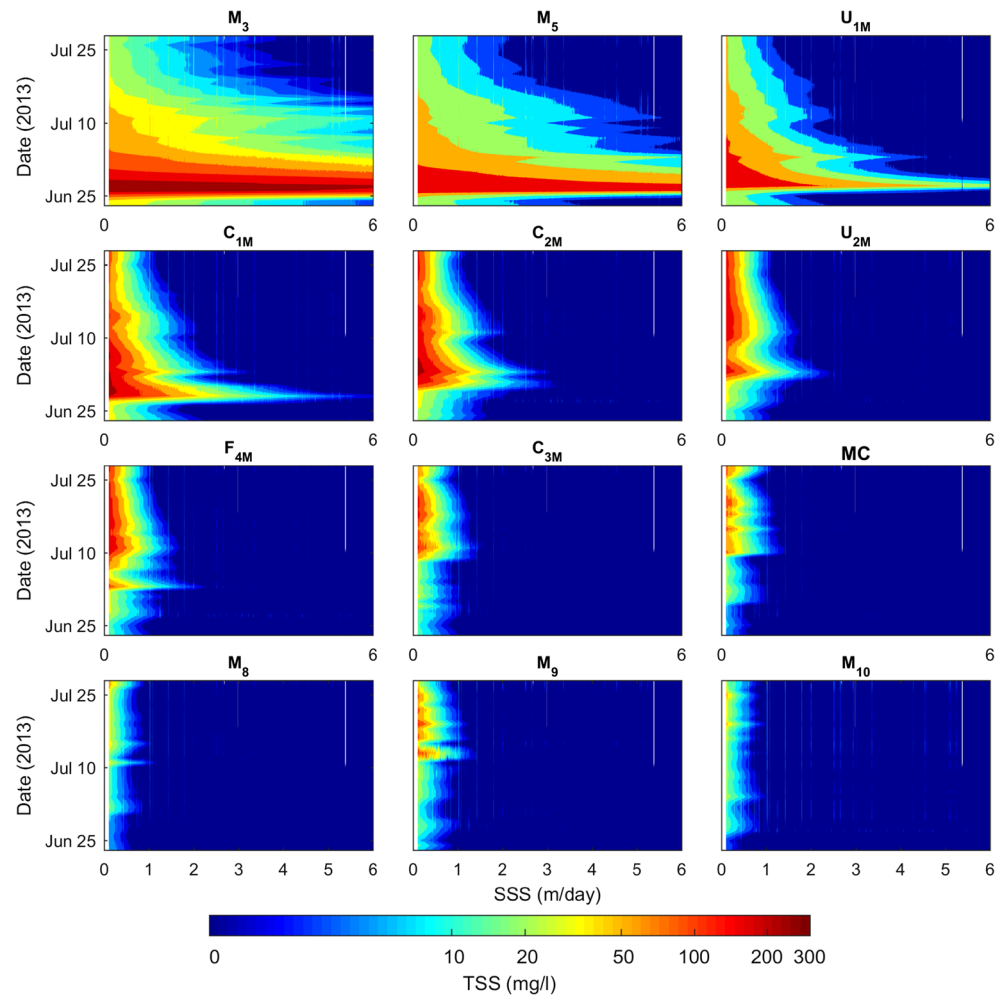
through sampling due to uncertainties inherent in measurement errors, spatiotemporal limits, and calculation limits. However, the model does extend our understanding of the overall responses of the system to different scenarios, particularly extremes.

In water quality modeling of lakes and reservoirs, the simulation errors can be reduced if the input data at the boundaries are well monitored (Romero and Imberger 2003). For having a correct image of the sediment transport by rivers, regular sampling programs are required (Walling 1977). Sediment rating curves can work as a replacement for sampling programs in case of financial austerity, missed events such as floods, and gaps of past sediment transport time series (Walling 1977). Turbidity measurements can also be used instead of directly measuring suspended solid concentrations. The turbidity measurements are highly affected by the particle size distribution of the suspended solids in water; hence, an adequate number of sampling is required when using the turbidity measurements with confidence, especially during flood events (Lenzi and Marchi 2000).

A large proportion of sediment transported in rivers is in the form of suspended solids; hence, sediment rating curves

which relate the suspended solid concentrations to the discharge values are commonly used for quantifying the amount of sediment transport in rivers and reservoirs (Asselman 2000). Although suspended solids make a large proportion of the total sediment load, the percentage is very variable along the river with greater variations at the headwaters and more consistent rates downstream (Lenzi and Marchi 2000). These changes can produce errors of up to 50% in estimating the sediment transport in rivers (Walling 1977). To reduce the uncertainties in determining the suspended solid concentrations and to have information on the characteristics of the sediment transport, different sediment rating curves are needed at various locations along rivers and reservoirs. The slopes of these rating curves provide information on the erosion and sedimentation rates in rivers, but not for all events. A study of the sediment rating curves of the Rhine River, Germany (Asselman 2000), found that the descending slopes of rating curves along the river do not influence the sediment transport rates. Due to data ownership limitations, the aim of this study was not to make a sediment rating curve based on the turbidity measurements, and the measured turbidity data were only used for the purpose of sediment model validation.

Accurate estimation of suspended solid concentrations with correct size distribution is essential at boundaries (Lee et al. 2007). Lack of input data could also be considered a limitation or even an opportunity for planning future studies. For example, we could potentially extract more information from the satellite images if there was a study looking into the relationship between the different bands in reflectance images and characteristics of SS such as particle size distribution and mineralogy. Having access to such a table would provide data at the inlet as input TSS and through the reservoir for calibration purposes. Also, it could reduce the need for using a variable settling coefficient inside the model, if we had a measure of sediment size distribution from linking the turbidity data to the corresponding TSS concentration by using sediment traps. The South Saskatchewan River (SSR) and Red Deer River (RDR) have considerable differences in the characteristics of the turbidity; the SSR has very clear water while the RDR has turbid water due to steep riverbed slopes. These two rivers merge in Saskatchewan only a few kilometer from the border of Alberta. In Saskatchewan, the general quality of water in the SSR was considered as "good" by the Saskatchewan Water Security Agency (WSA 2012); hence, fewer resources and water quality parameters were required for monitoring the quality of the water. The availability of water with an acceptable quality and less disturbance of the water resources by industrial activities and urbanization led to a very limited historical database of the water quality variables for the SSR and Lake Diefenbaker. One important factor which is missing in the model is river bank erosion, which is a very important source of sediment in Lake Diefenbaker (Ashmore and Day 1988). Bank erosion is different from sediment resuspension in bed material and could be imported into the model as TSS concentrations distributed over the upstream portion.

By using the turbidity as the only available data, a pronounced hurdle in the modeling was defining the suspended SSS. This parameter has a fixed value of meter per day, which is very restrictive, since, in actuality, the settling rates are extremely dependent on flow characteristics. In the example of LD (Figs. 8, 9, and 10), it can be clearly seen that larger settling rates are required as the reservoir becomes deeper and, consequently, the flow becomes slower. Comparing the TSS concentration at the LD inflow with the discharge and TSS at the SSR/RDR indicates that the TSS is more dependent on the flow than on the upstream concentration. Therefore, the current version of the CE-QUAL-W2 should only be used for sediment transport calculations of short time periods or for the systems with more uniform flow rates, unless the concentrations for different sediment classes are available. The model needs a more flexible sediment-settling coefficient that can differentiate between different sections of the river and reservoir.

The sensitivity results based on the Monte Carlo runs also demonstrate the need for using a dynamic SSS coefficient for an accurate sediment transport model (Fig. 8). RMSE values are higher upstream because TSS concentrations are larger at the reservoir inlet. Based on the available field measurements, the upstream concentrations are up to several times higher than those downstream. It is worth mentioning that the settling rates along the upstream areas are not actual sedimentation rates. The main reasons are that the model did not include the bank erosion rates, and only used one group of suspended solids in the simulations. In reality, bank erosion can contribute a significant portion to the sediment load. Also, the composition of the lake bed sediment and consequently the resuspension rates are different at different locations along the reservoir. Hence, the lower settling rates upstream are sedimentation rates reduced somewhat from the actual values to compensate for the simplifications in model setup. According to the RMSE values, the best results were obtained when SSS increased from 1 to 5 m/day from upstream to downstream in the reservoir. Based on our modeling results, the settling in the reservoir occurs more quickly than it does in the river because the flow velocity is smaller and the wind effects are dampened in the deeper layers. The settling rates increase even more downstream towards the dams. Also, because of suspended solids settling along the lake bed, the density gradient decreases down to the point that becomes smaller than the lake bed water density. At this stage, the sediment-laden water starts mixing with less turbid water at mid-layers and a larger proportion of the turbulent energy is used for mixing water vertically and laterally. As the head of the plume moves forward longitudinally, the laterally mixed waters have higher settling capacities.

Based on RMSE values, the results were not sensitive to τ_{cr} values (Fig. 8). However, this does not mean that the model also was not sensitive to this coefficient or the resuspension was not an important process. The reason is the overpredicting of the TSS by about two times at M_5 and about 15 times at U_{2M} when small values for SSS were selected in the model (Fig. 9). In that case, the values downstream were several times larger than the incoming TSS at the inlet, meaning that the extra TSS concentrations were from resuspension. The reason could be that the resuspended material was also affected by settling rates again and that would be why the SSS was more identifiable.

Conclusion

A water quality model was developed for Lake Diefenbaker to determine suspended solid transport and the rates of settling and resuspension through the reservoir. The length of the study was the 2 months of June and July 2013 when a flood occurred in the head waters of the SSR. The flood created the largest inflow to the reservoir since its construction in 1967, with flood waves carrying high loads of SS. We calibrated the

model based on measured turbidity data from 12 stations along Lake Diefenbaker collected during June and July 2013 and images obtained from cloud-free MODIS satellite imagery. We defined only one group of TSS because data on sediment texture (fine, medium, and coarse) were not available. TSS was modeled as a tracer, and its movement through the reservoir was traced starting at the upstream portion of Lake Diefenbaker, with the sediment plume gradually becoming less concentrated by sedimentation and dilution as it moved through the reservoir. This setup allowed us to develop a dispersion and diffusion transport model of Lake Diefenbaker using the two-dimensional hydrodynamic and water quality model CE-QUAL-W2. The model was capable of tracing the flood's sediment plume movements through the reservoir. This has resulted in a better understanding of the settling and resuspension rates of the SS in the reservoir which will support decision making.

The model results and turbidity measurements confirm that the inflow to the reservoir entered as an overflow and moved above the thermocline. Suspended solids were also transported by advection through the epilimnion, which was about 20 m at that time. As a result, the vertical alignment of suspended solids reversed with higher concentrations at the upper layers after the flooding. It took only a couple days for the plume to scatter throughout the reservoir, but took almost 1 month to disappear completely.

Satellite images were used to estimate the sediment's settling and resuspension rates by comparing the suspended solid transport with the sediment plume qualitatively. The turbidity in the upstream river is high, and it may be useful to apply wavelength studies to find correlations with TSS values. The narrow range of a few hundred meters is still a barrier, but improvements may become possible with higher-resolution satellite data in the future. Although a relationship between the reflectance bands from satellite images and the sediment concentrations was not available, the visible sediment plume movement provided good estimates of sediment transport in Lake Diefenbaker. The rates found confirmed those derived from the Monte Carlo results. This is a remarkable outcome considering that, in many cases, field measurements may not be available; however, other data sources may be successfully drawn upon to aid in calibration of such an event.

With the assumption of one single grain size, a limitation of the model was the lack of definition of the suspended SSS in the CE-QUAL-W2 model. This parameter has a fixed value, which is restrictive, since settling rates are extremely dependent on flow characteristics. However, good results were obtained by increasing settling rates in areas where the reservoir becomes deeper, and flow currents become slower. Therefore, the current version of the CE-QUAL-W2 model may be more suited for sediment transport calculations of shorter time periods and for systems with a uniform flow distribution. The model needs a more flexible sediment-settling coefficient that

at least differentiates between different sections of the river and reservoir.

More insight and confidence in the model could be obtained if several different data sources became available for model calibration. Finding correlations between reflectance bands from satellite images and sediment concentrations would considerably improve the quality of results. Also, finding the rates between the turbidity and corresponding TSS concentrations is essential for model validations. Input of SS distribution with a classification for different (fine, medium, and coarse) sizes is crucial. Finally, river bank erosion effects need to be considered in model calibrations.

References

Akomeah E, Chun KP, Lindenschmidt K-E (2015) Dynamic water quality modelling and uncertainty analysis of phytoplankton and nutrient cycles for the upper South Saskatchewan River. Environ Sci Pollut Res 22(22):18239–18251

Alavian V, Jirka GH, Denton RA, Johnson MC, Stefan HG (1992) Density currents entering lakes and reservoirs. J Hydraul Eng 118(11):1464–1489

Ashmore P, Day T (1988) Spatial and temporal patterns of suspended-sediment yield in the Saskatchewan River basin. Can J Earth Sci 25(9):1450–1463

Asselman NEM (2000) Fitting and interpretation of sediment rating curves. J Hydrol 234(3):228–248

Binding C, Bowers D, Mitchelson-Jacob E (2005) Estimating suspended sediment concentrations from ocean colour measurements in moderately turbid waters; the impact of variable particle scattering properties. Remote Sens Environ 94(3):373–383

Boehrer B, Schultze M, Ockenfeld K, Geller W (2005) Path of the 2002 Mulde flood through Lake Goitsche, Germany. Internationale Vereinigung fur Theoretische und Angewandte Limnologie Verhandlungen 29(1):369–372

Bolstad E (2016) Extreme floods may be the new normal. Available at: http://www.scientificamerican.com/ article/extreme-floods-may-be-the-new-normal/, Accessed: 3 October 2016

Buchak EM, Edinger JE (1984) Generalized, longitudinal-vertical hydrodynamics and transport: development, programming, and applications. Technical report, prepared for US Army Corps of Engineers Waterways Experiment Station, Vicksburg, MS

Budd JW, Warrington DS (2004) Satellite-based sediment and chlorophyll a estimates for Lake Superior. J Great Lakes Res 30:459–466

Cardenas MP, Schwab DJ, Eadie BJ, Hawley N, Lesht BM (2005) Sediment transport model validation in Lake Michigan. J Great Lakes Res 31(4):373–385

Cole TM, Buchak E (1995) *CE-QUAL-W2: a two-dimensional, laterally averaged, hydrodynamic and water quality model*. US Army Engineer Waterways Experiment Station, Vicksburg, MS, 2.0 edn

Cole TM, Wells SA (2003a) *CE-QUAL-W2: a two-dimensional, laterally averaged, hydrodynamic and water quality model*. US Army Engineer Waterways Experiment Station, Vicksburg, MS, 3.1 edn

Cole TM, Wells SA (2003b) *CE-QUAL-W2: a two-dimensional, laterally averaged, hydrodynamic and water quality model*. US Army Engineer Waterways Experiment Station, Vicksburg, MS, 3.2 edn

Cole TM, Wells SA (2006) *CE-QUAL-W2: a two-dimensional, laterally averaged, hydrodynamic and water quality model*. US Army Engineer Waterways Experiment Station, Vicksburg, MS, 3.5 edn

Cole TM, Wells SA (2008) *CE-QUAL-W2: a two-dimensional, laterally averaged, hydrodynamic and water quality model*. Department of Civil and Environmental Engineering, Portland State University, Portland, OR, 3.6 edn

Cole TM, Wells SA (2013) *CE-QUAL-W2: a two-dimensional, laterally averaged, hydrodynamic and water quality model*. Department of Civil and Environmental Engineering, Portland State University, Portland, OR, 3.71 edn

Cole TM, Wells SA (2015a) *CE-QUAL-W2: a two-dimensional, laterally averaged, hydrodynamic and water quality model*. Department of Civil and Environmental Engineering, Portland State University, Portland, OR, 3.72 edn

Cole TM, Wells SA (2015b) *CE-QUAL-W2: a two-dimensional, laterally averaged, hydrodynamic and water quality model*. Department of Civil and Environmental Engineering, Portland State University, Portland, OR, 4.0 edn

De Vynck G, Polson J (2013) Suncor among Calgary offices closed amid severe Alberta floods. Available at: http://business.financialpost.com/news/suncor-among-calgary-offices-closed-amid-severe-alberta-floods, Accessed: 3 October 2016

Derworiz C (2016) Southern Alberta flood leads to 'largest university-led water project in the world'. Available at: http://calgaryherald.com/news/national/southern-alberta-flood-leads-to-largest-university-led-water-project-in-the-world, Accessed: 3 October 2016

Dubourg P, North RL, Hunter K, Vandergucht DM, Abirhire O, Silsbe GM, Guildford SJ, Hudson JJ (2015) Light and nutrient co-limitation of phytoplankton communities in a large reservoir: Lake Diefenbaker, Saskatchewan, Canada. J Great Lakes Res 41:129–143

Eadie BJ, Schwab DJ, Johengen TH, Lavrentyev PJ, Miller GS, Holland RE, Leshkevich GA, Lansing MB, Morehead NR, Robbins JA et al (2002) Particle transport, nutrient cycling, and algal community structure associated with a major winter-spring sediment resuspension event in southern Lake Michigan. J Great Lakes Res 28(3):324–337

Edinger J, Buchak E (1975) *A hydrodynamic, two-dimensional reservoir model: the computational basis*. US Army Engineer Division, Ohio River. Cincinnati, OH

Edinger J, Buchak E (1978) Reservoir longitudinal and vertical implicit hydrodynamics. In: Proc. Int. Conf. on environmental effects of hydraulic engineering works, American society of civil engineers, Knoxville, TN

Fink G, Wessels M, Wüest A (2016) Flood frequency matters: why climate change degrades deep-water quality of peri-alpine lakes. J Hydrol 540:457–468

Giesy JP, Li PDS, Khim JS (2009) Water quality analysis report. Technical report, Toxicology Centre, University of Saskatchewan

Gippel CJ (1995) Potential of turbidity monitoring for measuring the transport of suspended solids in streams. Hydrol Process 9(1):83–97

Grove JR, Croke J, Thompson C (2013) Quantifying different riverbank erosion processes during an extreme flood event. Earth Surf Process Landf 38(12):1393–1406

Hecker M, Khim JS, Giesy JP, Li S-Q, Ryu J-H (2012) Seasonal dynamics of nutrient loading and chlorophyll a in a northern prairies

reservoir, Saskatchewan, Canada. Journal of Water Resource and Protection 4(04):180

Horritt M (2006) A methodology for the validation of uncertain flood inundation models. J Hydrol 326(1):153–165

Huber A, Ivey GN, Wake G, Oldham CE (2008) Near-surface wind-induced mixing in a Mine Lake. J Hydraul Eng 134(10):1464–1472

Hudson JJ, Vandergucht DM (2015) Spatial and temporal patterns in physical properties and dissolved oxygen in Lake Diefenbaker, a large reservoir on the Canadian Prairies. J Great Lakes Res 41:22–33

Ji Z-G (2008) Hydrodynamics and water quality: modeling rivers, lakes, and estuaries. John Wiley & Sons

Klemm W, Greif A, Broekaert JA, Siemens V, Junge FW, Van der Veen A et al (2005) A study on arsenic and the heavy metals in the Mulde river system. CLEAN–Soil, Air, Water 33(5):475–491

Kroon FJ, Kuhnert PM, Henderson BL, Wilkinson SN, Kinsey-Henderson A, Abbott B, Brodie JE, Turner RD (2012) River loads of suspended solids, nitrogen, phosphorus and herbicides delivered to the Great Barrier Reef lagoon. Mar Pollut Bull 65(4):167–181

Langeveld J, Veldkamp R, Clemens F (2005) Suspended solids transport: an analysis based on turbidity measurements and event based fully calibrated hydrodynamic models. Water Sci Technol 52(3):93–101

Lee C, Schwab DJ, Hawley N (2005) Sensitivity analysis of sediment resuspension parameters in coastal area of southern Lake Michigan. Journal of Geophysical Research: Oceans 110(C3). doi:10.1029/2004JC002326

Lee C, Schwab DJ, Beletsky D, Stroud J, Lesht B (2007) Numerical modeling of mixed sediment resuspension, transport, and deposition during the March 1998 episodic events in southern Lake Michigan. Journal of Geophysical Research: Oceans 112(C2). doi:10.1029/2005JC003419

Lenzi MA, Marchi L (2000) Suspended sediment load during floods in a small stream of the Dolomites (northeastern Italy). Catena 39(4):267–282

Littlewood IG (1992) Estimating contaminant loads in rivers: a review. Institute of Hydrology (Centre for Ecology & Hydrology), Crowmarsh Gifford, Wallingford, Oxfordshire, OX1O 8BB

Liu G, Zhu J, Wang Y, Wu H, Wu J (2011) Tripod measured residual currents and sediment flux: impacts on the silting of the Deepwater Navigation Channel in the Changjiang Estuary. Estuar Coast Shelf Sci 93(3):192–201

Mama C, Okafor F (2011) Siltation in reservoirs. Nigerian Journal of Technology 30(1):85–90

Myint S, Walker N (2002) Quantification of surface suspended sediments along a river dominated coast with NOAA AVHRR and SeaWiFS measurements: Louisiana, USA. Int J Remote Sens 23(16):3229–3249

Pappenberger F, Matgen P, Beven KJ, Henry J-B, Pfister L, Fraipont P (2006) Influence of uncertain boundary conditions and model structure on flood inundation predictions. Adv Water Resour 29(10):1430–1449

Romero JR, Imberger J (2003) Effect of a flood underflow on reservoir water quality: data and three-dimensional modeling. Arch Hydrobiol 157(1):1–25

Sadeghian A, Hudson J, Wheater H, Lindenschmidt K (2014) Water quality modeling of Lake Diefenbaker. Water news Can Water Res Assoc 33(2):17–20

Sadeghian A, de Boer D, Hudson JJ, Wheater H, Lindenschmidt K-E (2015) Lake Diefenbaker temperature model. J Great Lakes Res 41:8–21

Sakmont Engineering (1987) A satellite imagery survey of land use in the effective drainage area of the South Saskatchewan River Basin. technical report d.2. Technical report, Consulting Hydraulic Engineers. Saskatoon, Saskatchewan

Saskatoon City News (2013) 2013 high river flow updates. Available at: www.saskatooncitynews.ca, Accessed: 28 June 2013

Stroud JR, Lesht BM, Schwab DJ, Beletsky D, Stein ML (2009) Assimilation of satellite images into a sediment transport model of Lake Michigan. Water Resour Res 45(2). doi:10.1029/2007WR006747

Surbeck CQ, Jiang SC, Ahn JH, Grant SB (2006) Flow fingerprinting fecal pollution and suspended solids in stormwater runoff from an urban coastal watershed. Environmental science & technology 40(14):4435–4441

Sutherland S (2016) Three years later: what caused the 2013 Alberta floods? Available at: https://www.theweathernetwork.com/news/articles/why-was-southern-alberta-so-vulnerable-to-flooding-in-2013/29800, Accessed: 3 October 2016

Valero-Garces BL, Navas A, Machin J, Walling D (1999) Sediment sources and siltation in mountain reservoirs: a case study from the central Spanish pyrenees. Geomorphology 28(1):23–41

Vincent WF, Gibbs MM, Spigel RH (1991) Eutrophication processes regulated by a plunging river inflow. Hydrobiologia 226(1):51–63

Walling DE (1977) Limitations of the rating curve technique for estimating suspended sediment loads, with particular reference to British rivers. Erosion and solid matter transport in inland waters. IAHS Publ 122:34–48

Welsch E, De Vynck G (2013) Alberta floods spread as water subsides in Calgary. Available at: http//www.bloomberg.com/news/articles/2013-06-24/alberta-floods-spread-as-water-subsides-in-oil-hub-of-calgary, Accessed: 3 October 2016

Wetzel RG (2001) Limnology: lake and river ecosystems. Gulf Professional Publishing. 3rd edn

Wheater H, Evans E (2009) Land use, water management and future flood risk. Land Use Policy 26:S251–S264

Wheater H, Gober P (2013) Water security in the Canadian Prairies: science and management challenges. Philosophical Transactions of the Royal Society of London A: Mathematical, Physical and Engineering Sciences 371(2002):20120409

WSA (2012) State of lake diefenbaker. Water Security Agency. Available at: https://www.wsask.ca/Global/Lakes%20and%20Rivers/Dams%20and%20Reservoirs/Operating%20Plans/Developing%20an%20Operating%20Plan%20for%20Lake%20Diefenbaker/State%20of%20Lake%20Diefenbaker%20Report%20-%20October%2019%202012.pdf, Accessed: 21 May 2015

Wüest A, Imboden DM, Schurter M (1988) Origin and size of hypolimnic mixing in Urnersee, the southern basin of Vierwaldstättersee (Lake Lucerne). Schweizerische Zeitschrift für Hydrology 50(1):40–70

Yip H (2015) An assessment of present and historical (1984–2012) Lake Diefenbaker water clarity and chlorophyll-a concentration using Landsat imagery. Master's thesis, University of Saskatchewan